Noble 2D Materials

DOI: 10.1002/anie.201309280

Two Dimensional Materials Beyond MoS_2: Noble-Transition-Metal Dichalcogenides**

Pere Miró, Mahdi Ghorbani-Asl, and Thomas Heine**

Abstract: *The structure and electronic structure of layered noble-transition-metal dichalcogenides MX_2 (M = Pt and Pd, and chalcogenides X = S, Se, and Te) have been investigated by periodic density functional theory (DFT) calculations. The MS_2 monolayers are indirect band-gap semiconductors whereas the MSe_2 and MTe_2 analogues show significantly smaller band gap and can even become semimetallic or metallic materials. Under mechanical strain these MX_2 materials become quasi-direct band-gap semiconductors. The mechanical-deformation and electron-transport properties of these materials indicate their potential application in flexible nanoelectronics.*

During the first decades of the 20th century, the scientific community concluded that two dimensional (2D) materials did not exist.[1,2] These materials were thought to be thermodynamically unstable and consequently would not exist at any finite temperature. Their arguments were based on the effect of thermal fluctuations observed experimentally in thin films.[3] Against all odds, Novoselov and Geim were able to isolate the first 2D material in 2004, individual graphene layers, just by using adhesive tape.[4,5] This discovery was the starting point for a completely new field that has led to the synthesis of many 2D materials during the last decade.[6–11]

Layered transition-metal chalcogenide (TMC) nanostructures, even though known and studied for a long time, are now rapidly emerging as they display unique chemical and physical properties that are absent or difficult to obtain in other 2D materials, such as graphene.[10] For example, in graphene, complex band-gap engineering is required for its application as a transistor. In contrast, many TMCs are inherent semiconductors by nature.[12] In consequence, a wide range of applications, such as electronics, optoelectronics, photovoltaics, and catalysis[13–15] have been demonstrated to be possible for these materials. Even though, there are many TMCs that have remained almost unexplored, and understanding of the physics behind these systems is fundamental towards their development and practical application.

The layered crystal structure of noble TMCs has been known since the work of Grønvold et al. and Kjekshus et al. on $PdS_2/PdSe_2$ and $PtS_2/PtSe_2$, respectively.[16–18] The electronic structure of platinum TMC materials was subject of a controversial debate in the scientific community in the 1970s, concluding that sulfides and selenides were semiconducting.[19] The exfoliation and subsequent application of these materials is still in it's infancy since the economic cost of noble metals limits large-scale applicability. However, for their use as a monolayer material the material cost is less significant and should not restrict their application for specific nanoelectronic applications (e.g. TMC-based contacts or transistors).

Herein, we report a study of the electronic structure of mono- and bilayers, strain effects and the conductance of these materials. We have considered layered TMCs of general formula MX_2, where M is a noble metal (Pd or Pt) and X is a chalcogenide element (S, Se and Te; Figure 1). Even though nickel is not a noble metal and it does not form layered TMCs, it has been considered in this work since several 3D materials have been found to form 2D materials under certain conditions.[20] For all MX_2 materials, the reported crystal structures have two polytypes: 2O and 1T. At the monolayer limit, 1T is thermodynamically favored and in consequence, the only one presented herein (see the Supporting Information for the other polytype). The layered structures were cut out from the bulk structures in the direction of the layer

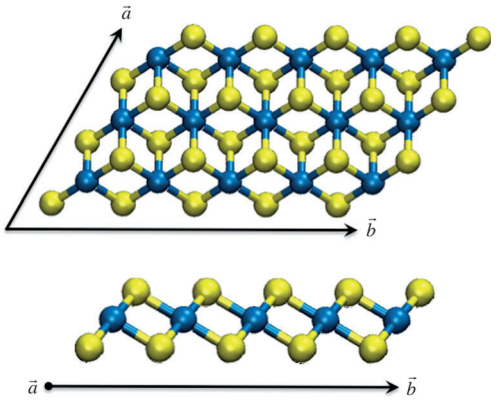

Figure 1. Top and side view of the transition-metal dichalcogenides structures (MX_2) studied. Metal center (M = Ni, Pd, or Pt) blue and chalcogenide (X = S, Se, or Te) yellow.

[*] Dr. P. Miró, M. Ghorbani-Asl, Prof. Dr. T. Heine
School of Engineering and Science, Jacobs University Bremen
28759 Bremen (Germany)
E-mail: p.miro@jacobs-university.de
t.heine@jacobs-university.de

[**] This work was supported by the German Research Council (Deutsche Forschungsgemeinschaft, HE 3543/18-1), The European Commission (FP7-PEOPLE-2009-IAPP QUASINANO, GA 251149 and FP7-PEOPLE-2012-ITN MoWSeS, GA 317451), and ONRG (N62909-13-1-N222 ONR (UK)). We thank Dr. Augusto Oliveira and Mohammad Wahiduzzaman for the DFTB parameters, and Nourdine Zibouche for inspiring discussions.

Supporting information for this article is available on the WWW under http://dx.doi.org/10.1002/anie.201309280.

stacking (001). The full computational details are given in the Supporting Information. In summary, we have used periodic density functional theory (DFT) calculations with the dispersion corrected Perdew-Burke-Ernzerhof exchange-correlation functional (PBE-D) with the triple-ζ basis set plus a polarization functions (TZP) on all atoms.[21,22] Single point calculations were performed using TB-BJ and GLLB-SC models.[23,24]

Our calculations show that all of the studied transition-metal disulfide monolayers are indirect-gap semiconductors with band gaps of 0.51, 1.11, and 1.75 eV for NiS_2, PdS_2, and PtS_2, respectively (Figure 2a). Our results are in the low band-

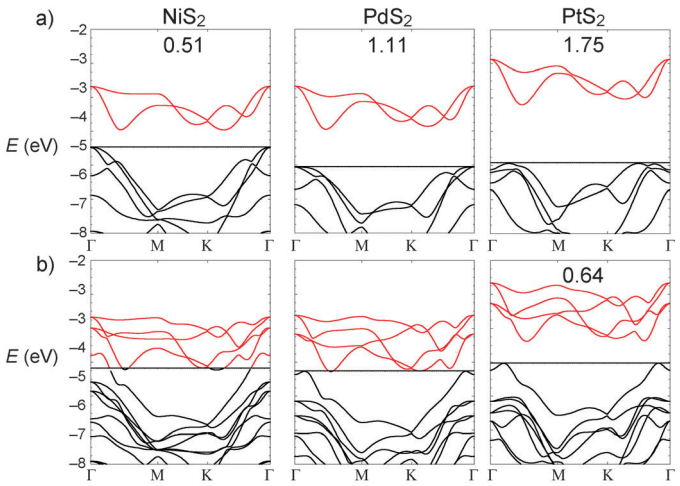

Figure 2. Band structure of the studied TMC monolayers (a) and bilayers (b) calculated at the DFT/PBE-D level. The band gap (in eV) is indicated in each band structure. The horizontal lines indicate the Fermi level. Valence band (black), conduction band (red).

gap range, as reported at a similar level of theory for other semiconductor TMC monolayers (except for PdS_2); however, the chosen level of theory has a major influence on the computed band gap.[25–27] The GLLB-SC model potential enables an improved and fast quasi-particle band-gap calculation that includes the derivative discontinuity that is lacking in PBE. This term increases the NiS_2, PdS_2, and PtS_2 band gaps to 0.79, 1.67, and 2.72 eV, respectively, with no changes in the overall shape of the band structures. GLLB-SC results are comparable to GW calculations and analogously are subject to the strong excitonic effect in 2D materials. In consequence, these methods tend to overestimate TMC band gaps.[28] As PBE generally underestimates electronic band gaps, we can safely assume the correct values being between the PBE and the GLLB-SC results and close to the ones determined by the TB-BJ model which are 0.50, 1.17, and 1.90 eV for the NiS_2, PdS_2, and PtS_2, respectively. TB-BJ results confirm the validity of PBE to study these materials.

The fundamental band gap originates from a transition from the top of the valence band situated at Γ to the bottom of the conduction band halfway between the Γ and M high-symmetry points (Figure 2a). The only exception is PtS_2, where there are two degenerate areas in the top of the valence band. The optical direct band gap is always situated halfway between the Γ and M high-symmetry points and for PtS_2 close to the value of the indirect band gap (Figure 2a). When a 1T bilayer is considered, the band gap is greatly decreased. The NiS_2 and PdS_2 bilayers become metallic, while the band gap in PtS_2 decreases to 1.1 eV (Figure 2b).[25] The interlayer interaction energy grows stronger when moving down in the periodic table (Ni, Pd, Pt), with interaction energies ranging from 45 to 130 meV per MX_2 unit, in agreement with the values reported by Xu et al.[29] Vertical confinement effects observed in noble TMCs are analogous to those observed in WS_2 and MoS_2, but stronger.

Tensile stress and compression of the monolayers, force changes to the positions of the atoms while also inducing changes in the electronic structure and other properties. TMCs can be exposed to strong mechanical deformations without reaching their fracture point because the M–X bonds and X-M-X bond angles they contain are very flexible. We applied uniaxial (along $\vec{a}$) and biaxial (2D isotropic) strains of up to 10% to all of the materials studied.[30] Figure 3 shows the band-gap evolution with the applied uniaxial and isotropic deformation for the MS_2 monolayers at the PBE level of theory.

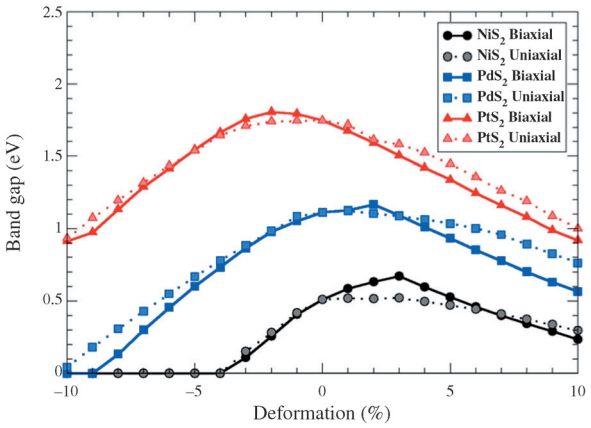

Figure 3. Band gap at PBE levels of theory of NiS_2, PdS_2, and PtS_2 at different uniaxial (dashed lines) and biaxial (solid lines) compression or strain percentages.

In equilibrium, the noble MS_2 monolayers are indirect band-gap semiconductors. Under tensile strain, a point in the Brillouin zone halfway between the Γ and M high-symmetry points rapidly becomes the top of the valence band and its prominence seems to be proportional to the applied strain (Figure 4). The uniaxial compression or stretch of these materials leads to the reduction their band gap, while under biaxial stretch deformations, the band gap in NiS_2 and PdS_2 monolayers increases by 0.15 eV at 2–3% strain before decreasing, while in PtS_2 the band gap always decreases proportionally with the strain. We extrapolated the point at which the band gap vanishes under biaxial elongations to about 14% (NiS_2), 18% (PdS_2), and 22% (PtS_2), at this point the monolayers become metallic with bands crossing the Fermi level. However, further experiments are needed to

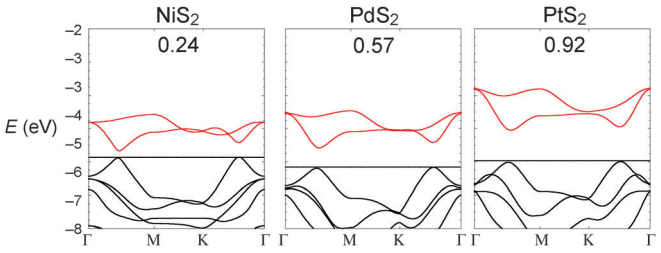

Figure 4. Band structure of the studied TMC monolayers under 10% biaxial strain calculated at the DFT/PBE-D level. The band gap (in eV) is indicated in each band structure. The horizontal lines indicate the Fermi level. Valence band (black), conduction band (red).

better perceive the stiffness and exact rupture point of these materials as other TMC have their rupture point at maximum strain of about 15%.[31] Similar behavior is observed when a monolayer is exposed to compressive strain, though the top of valence band is situated at the Γ point while the nature of the bottom of the conduction band remains unchanged. The biaxial compression of NiS_2 and PdS_2 monolayers always decreases the band gap, but in PtS_2 it increases slightly up to a compression of 2%. In every case, a change from an indirect to quasi direct band gap semiconductor is observed. The band structures of the stretched materials indicate a decrease in the phonon energy required for an electronic excitation because, with the stretching, the materials change into semiconductors with a quasi-direct band gap (Figure 4).

The noble-transition-metal diselenide monolayers have similar band structures with small band gaps; for $PdSe_2$ and $PtSe_2$ they are as low as 0.39 and 1.05 eV, respectively. In contrast ditellurides are semimetals (see the Supporting Information for details). No significant changes in the band gap or the band structure were observed in any of the studied materials when spin-orbit effects were considered.

The geometry changes caused by to applied deformations are need to be elastic, to allow the materials to undergo reversible linear stretching–compression behavior in compliance with Hooke's law (see the Supporting Information for the calculated stress–strain curves up to 10% deformation), they relax to their equilibrium structures once the stress is released. This result indicates that we are in the elastic region and demonstrates the ductility of these materials. Fitting these stress–strain curves gives the corresponding elastic modulus of each material. Both uniaxial and biaxal fitted Young's moduli for the studied materials are presented in Table S24. The uniaxial elastic modulus of NiS_2, PdS_2, and PtS_2 monolayers are 272, 245, and 335 GPa, respectively. To our knowledge, there are no measurements of the elastic modulus on these materials; however, our results are the same order of magnitude as those determined in other TMCs, such as MoS_2 (195 GPa) and WS_2 (214 GPa), and well below that of graphene (2400 GPa).[32–34] Biaxial deformations lead to higher elastic moduli values. In all the cases, the presence of larger chalcogenide atoms leads to a more flexible material.

The electron conductance of the semiconducting monolayers was calculated self-consistently using the Green's function formalism together with the density functional based tight-binding method.[35–38] Both compression and strain induce minor changes in the conductance of the studied monolayers, while the main features remain completely unaltered (see the Supporting Information). Our results demonstrate that noble TMCs preserve their conductance under uniaxial and biaxial strains.

In conclusion, we revealed that at the monolayer level noble TMCs are indirect band-gap semiconductors, however these materials may become metallic as a result of vertical confinement effects. The calculated elastic moduli of these materials are larger than those of MoS_2 and WS_2 monolayers, but still significantly lower than that of graphene. Strain effects have been suggested as a possible way of tuning band gaps without large changes in the transport properties of noble TMC monolayers. Furthermore, the mechanical stretch of these materials decreases the phonon energy required for the electronic excitation in indirect band-gap semiconductors. This property opens new perspectives for the application of these materials in flexible nanodevices. However, further studies are required to fully understand and control these materials towards their application in optoelectronics or nanosensor device engineering.

Further studies are ongoing in our group to study nanotubes based on the materials reported herein as well as on the effects of doping and defects on the electronic structure of the studied systems.

Received: October 24, 2013
Published online: February 19, 2014

Keywords: 2D materials · chalcogenides · noble metals · palladium · platinum

[1] a) E. M. Lifshitz, L. P. Pitaevskii, *Statistical Physics Part I*, Pergamon, Oxford, **1980**; b) L. D. Landau, E. M. Lifshitz, L. P. Pitaevskii, *Statistical Physics Part II*, Pergamon, Oxford, **1980**.
[2] a) R. E. Peierls, *Ann. Inst. Henri Poincare* **1935**, *5*, 177; b) R. E. Peirls, *Helv. Phys. Acta* **1934**, *7*, 81.
[3] N. D. Mermin, H. Wagner, *Phys. Rev. Lett.* **1966**, *17*, 1133.
[4] K. S. Novoselov, A. K. Geim, S. V. Morozov, D. Jiang, Y. Zhang, S. V. Dubonos, I. V. Grigorieva, A. A. Firsov, *Science* **2004**, *306*, 666.
[5] K. S. Novoselov, A. K. Geim, S. V. Morozov, D. Jiang, M. I. Katsnelson, I. V. Grigorieva, S. V. Dubonos, A. A. Firsov, *Nature* **2005**, *438*, 197.
[6] D. Pacile, J. C. Meyer, C. O. Girit, A. Zettl, *Appl. Phys. Lett.* **2008**, 92.
[7] J. C. Meyer, A. Chuvilin, G. Algara-Siller, J. Biskupek, U. Kaiser, *Nano Lett.* **2009**, *9*, 2683.
[8] J. N. Coleman, M. Lotya, A. O'Neill, S. D. Bergin, P. J. King, U. Khan, K. Young, A. Gaucher, S. De, R. J. Smith, I. V. Shvets, S. K. Arora, G. Stanton, H. Y. Kim, K. Lee, G. T. Kim, G. S. Duesberg, T. Hallam, J. J. Boland, J. J. Wang, J. F. Donegan, J. C. Grunlan, G. Moriarty, A. Shmeliov, R. J. Nicholls, J. M. Perkins, E. M. Grieveson, K. Theuwissen, D. W. McComb, P. D. Nellist, V. Nicolosi, *Science* **2011**, *331*, 568.
[9] M. Chhowalla, H. S. Shin, G. Eda, L. J. Li, K. P. Loh, H. Zhang, *Nat. Chem.* **2013**, *5*, 263.
[10] Q. H. Wang, K. Kalantar-Zadeh, A. Kis, J. N. Coleman, M. S. Strano, *Nat. Nanotechnol.* **2012**, *7*, 699.
[11] A. Pakdel, Y. Bando, D. Golberg, *Chem. Soc. Rev.* **2014**, *43*, 934.

[12] K. F. Mak, C. Lee, J. Hone, J. Shan, T. F. Heinz, *Phys. Rev. Lett.* **2010**, *105*, 136805.
[13] H. Topsøe, B. S. Clausen, F. E. Massoth, *Hydrotreating Catalysis, Science and Technology*, Springer, Berlin, **1996**.
[14] J. V. Lauritsen, M. Nyberg, J. K. Norskov, B. S. Clausen, H. Topsoe, E. Laegsgaard, F. Besenbacher, *J. Catal.* **2004**, *224*, 94.
[15] S. Gemming, G. Seifert, *Nat. Nanotechnol.* **2007**, *2*, 21.
[16] F. Grønvold, E. Rost, *Acta Chem. Scand.* **1956**, *10*, 1620.
[17] A. Kjekshus, F. Grønvold, *Acta Chem. Scand.* **1959**, *13*, 1767.
[18] F. Grønvold, H. Haraldsen, A. Kjekshus, *Acta Chem. Scand.* **1960**, *14*, 1879.
[19] J. A. Wilson, A. D. Yoffe, *Adv. Phys.* **1969**, *18*, 193.
[20] C. Tusche, H. L. Meyerheim, J. Kirschner, *Phys. Rev. Lett.* **2007**, *99*, 26102.
[21] J. P. Perdew, K. Burke, M. Ernzerhof, *Phys. Rev. Lett.* **1996**, *77*, 3865.
[22] ADF2012, SCM, Theoretical Chemistry, Vrije Universiteit, Amsterdam, The Netherlands, http://www.scm.com.
[23] M. Kuisma, J. Ojanen, J. Enkovaara, T. T. Rantala, *Phys. Rev. B* **2010**, *82*, 115106.
[24] F. Tran, P. Blaha, *Phys. Rev. Lett.* **2009**, *102*, 226401.
[25] A. Kuc, N. Zibouche, T. Heine, *Phys. Rev. B* **2011**, *83*, 245213.
[26] K. F. Mak, C. Lee, J. Hone, J. Shan, T. F. Heinz, *Phys. Rev. Lett.* **2010**, *105*, 136805.
[27] W. Li, C. F. J. Walther, A. Kuc, T. Heine, *J. Chem. Theory Comput.* **2013**, *9*, 2950.
[28] M. Kuisma, J. Ojanen, J. Enkovaara, T. T. Rantala, *Phys. Rev. B* **2010**, *82*, 115106.
[29] M. Xu, T. Liang, M. shi, H. Chen, *Chem. Rev.* **2013**, *113*, 3766.
[30] Compression of the freestanding monolayer is hypothetical, as the material would bend in the direction normal to the 2D crystal plane.
[31] I. Kaplan-Ashiri, S. R. Cohen, K. Gartsman, V. Ivanovskaya, T. Heine, G. Seifert, I. Wiesel, H. D. Wagner, R. Tenne, *Proc. Natl. Acad. Sci. USA* **2006**, *103*, 523.
[32] M. Ghorbani-Asl, S. Borini, A. Kuc, T. Heine, *Phys. Rev. B* **2013**, *87*, 235434.
[33] P. Miró, M. Ghorbani-Asl, T. Heine, *Adv. Mater.* **2013**, *25*, 5366.
[34] J.-U. Lee, D. Yoon, H. Cheong, *Nano Lett.* **2012**, *12*, 4444.
[35] D. S. Fisher, P. A. Lee, *Phys. Rev. B* **1981**, *23*, 6851.
[36] M. P. L. Sancho, J. M. L. Sancho, J. Rubio, *J. Phys. F* **1985**, *15*, 851.
[37] S. Datta, *Quantum Transport: Atom to Transistor, 2nd ed.*, Cambridge University Press, Cambridge/New York, **2005**.
[38] M. Wahiduzzaman, A. F. Oliveira, P. Philipsen, L. Zhechkov, E. van Lenthe, H. A. Witek, T. Heine, *J. Chem. Theory Comput.* **2013**, *9*, 4006.

